ACS Biomaterials SCIENCE & ENGINEERING

pubs.acs.org/journal/abseba

Article

De Novo Synthesis of Elastin-like Polypeptides (ELPs): An Applied Overview on the Current Experimental Techniques

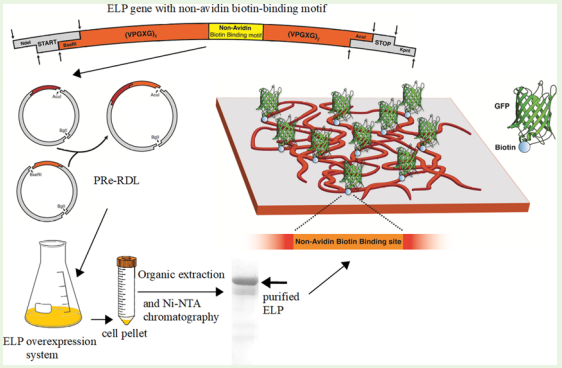
Ioannis G. Riziotis,[†] Paraskevas Lamprou,[†] Eleni Papachristou, Aglaia Mantsou, Georgios Karolidis, Rigini Papi, and Theodora Choli-Papadopoulou*

Cite This: *ACS Biomater. Sci. Eng.* 2021, 7, 5064−5077

Read Online

ACCESS | Metrics & More | Article Recommendations | Supporting Information

ABSTRACT: Elastin-like polypeptides (ELPs) are protein-based biopolymers genetically produced from polypeptides composed of a repeating pentapeptide sequence V−P−G−X−G. The inherent properties of recombinant ELPs, such as smart nature, controlled sequence complexity, physicochemical properties, and biocompatibility, make these polymers suitable for use in nanobiotechnological applications, as biofunctionalized scaffolds for tissue-engineering purposes and drug delivery. In this work, we report the design and synthesis of two elastomeric self-assembling polypeptides (ELPs) that mimic the endogenous human tropoelastin. Using molecular biology techniques, two artificial genes that encode two ELP concatemers of approximate molecular mass 60 kDa, one of them carrying biotin-binding peptide motifs, were constructed. These motifs could facilitate biofunctionalization of the ELPs through tethering biotinylated factors, such as growth factors. The ELPs were heterologously overexpressed in *E. coli* and subsequently purified in two steps: a nonchromatographic technique by organic solvent extraction, followed by nickel−nitrilotriacetic acid (Ni-NTA) affinity chromatography. The characterization of the biochemical properties and biocompatibility of ELPs was also performed in this study. The ELP carrying the biotin-binding motifs was tested for its capability to bind biotin, and indeed, it was observed that it can bind biotinylated proteins specifically. Additionally, results concerning the cytotoxicity of the ELPs exhibited excellent compatibility of the ELPs with mammalian cells in vitro. We anticipate that these ELPs can be used as components of a scaffold that mimics the extracellular matrix (ECM) for the regeneration of endogenously highly elastic tissues.



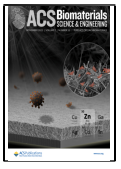
KEYWORDS: *non-avidin, concatemers, biocompatibility, scaffolds, biofunctionalization*

1. INTRODUCTION

Mammalian elastin is an extensively studied biopolymer in terms of sequence and structure, with artificial materials mimicking its properties being developed for biotechnological applications. Isolating and processing endogenous elastin is a difficult task because of the insolubility of the molecules[1]; thus, de novo design and synthesis of similar molecules is the most feasible approach to utilize the chemical and mechanical properties of elastin in composite biomaterials.[2] Such designed polypeptides were first introduced by Urry et al.[3,4] in 1974 and are known as elastin-like polypeptides (ELPs). They consist of tandem repeats of the basic tropoelastin linear sequence motif VPGXG, where residue X in the 4th position is a variable residue (guest residue). ELPs have been proven useful in biomedical applications and are widely a part of the nanobiotechnology toolkit in the development of biomimicking materials for regenerative medicine, tissue engineering, and drug delivery.[5] The reasons why ELPs find applicability in these fields are the capability of precise tuning of their physicochemical properties, biofunctionalization through incorporating specific linear motifs in their sequence (e.g., lysine-glycine-aspartate (RGD) integrin-binding motifs for cell adhesion),[6−8] as well as their biocompatibility.[9] The comparative advantage of ELPs against endogenous elastin is their solubility in aqueous environments while retaining the property of self-assembly into flexible polymer structures through a reversible thermal-phase-transition process.[10]

As stated above, an ELP sequence mainly consists of the $(VPGXG)_n$ repeated motif; the number of repeats n and the sequence composition in guest residues X are the most important factors directly affecting the thermal and mechanical properties of ELPs. The typical variable attribute of ELPs dependent on the factors mentioned above is critical

Received: March 9, 2021
Accepted: June 21, 2021
Published: October 20, 2021



Downloaded from pubs.acs.org/abseba/article-pdf/7/11/5064/3413050/ab1c00329.pdf by guest on 12 November 2026

ACS Publications

© 2021 The Authors. Published by American Chemical Society

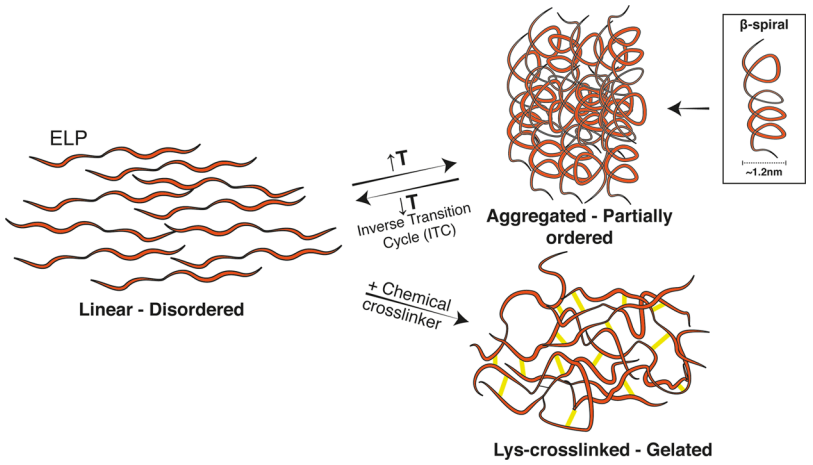


Figure 1. Structural transitions of ELPs. An endogenous property of ELPs is the temperature-dependent reversible-phase transition from linear, disordered coils to partially ordered β-spirals of ~1.2 nm diameter that can self-assemble into aggregates, upon the increase in environment temperature. Also, the treatment of ELPs with a chemical cross-linker makes it possible to irreversibly form an elastin-mimicking hydrogel structure by covalent bonding between the side chains of Lys residues introduced in the guest-residue position of the ELP-repeating motif VPGXG.

temperature T_t, at which the molecules undergo structural transition. In environment temperatures below T_t, hydrophobic side-chain groups are surrounded by water molecules, making ELPs linear and soluble. By increasing temperature beyond T_t, the formation of β-structures is thermodynamically favored, and ELPs self-assemble into β-spiral secondary structures. This transition from a soluble random coil, disordered state to a partially ordered state[11] can be described as temperature-dependent phase transition. By modifying the sequence and length of ELPs, it is possible to tune T_t in a predictable manner; however, other factors such as buffer ion strength and the presence of chaotropic or cosmotropic salts could affect intermolecular interactions among ELPs and change the critical temperature.[12] ELPs can be used as the primary component to build gridlike structures (i.e., hydrogels) that could function as cell-cultivation scaffolds. By introducing Lys residues in the guest-residue positions of the VPGXG motifs, it is possible to perform chemical cross-linking between these residues, forming covalently linked ELP network structures. Interestingly, ELPs maintain their thermal-phase-transition capability even in their cross-linked form.[3,5,12,13] The two structural traits described in this paragraph are presented schematically in Figure 1.

For most regenerative medicine applications for which ELPs are used, it is crucial to design cost-effective protocols for the production of recombinant ELPs of high purity in high yields, while retaining all physicochemical properties. In this work, we report a detailed protocol for the design, synthesis, and purification of ELPs based on DNA-concatemerization methods, such as polymerase chain reaction (PCR)-based DNA ligation,[14] recursive directional ligation by plasmid reconstruction (Pre-RDL),[15,16] and a nonchromatographic protein-purification technique by organic solvent extraction[17] that have been previously described. To be more specific, this protocol was used for the construction, purification, and partial characterization of a novel ELP of ~60 kDa molecular mass that contains motifs that can bind biotin and whose amino-acid sequence bears no resemblance to those of avidin or streptavidin (non-avidin-related biotin-binding motifs—NAVs).[18] Currently, we tested whether a biotinylated protein, such as biotinylated green fluorescent protein (GFP), could be tethered to the NAVs introduced into the ELP specifically, as well as the cytotoxicity of the ELP. These NAV motifs can be potentially used as binding sites for biotinylated protein factors to facilitate biofunctionalization of ELPs. Downstream, biofunctionalized ELPs could be used in the future for biomedical applications, for instance, as components of tissue-engineering scaffolds (for bones, cartilages, tendons, skin tissues, and so forth.[19]) or as drug carriers for drug delivery.[20,21] Our future goal is the pilot development of a postsynthesis biofunctionalization system, with the first step to design and synthesize simple, biotin-compatible ELP polymers that can self-assemble. By making use of the versatile system of in vivo biotinylation,[22,23] it is possible to on-demand functionally modify three-dimensional (3D) cell-culture scaffolds that contain ELPs (for example, by incorporating a growth factor or a part of it), thus creating "smart" materials of biomedical interest. Furthermore, with the design and production of simple ELP molecules such as the ones described in this study, we seek to construct a protocol containing all steps of production using known techniques, from the design to purification and some partial characterization.

2. METHODS

2.1. ELP Gene-Construction Step 1—PCR-Based Synthesis. Monomer ELP genes (NAV-ELP$_1$ and CTRL-ELP$_1$) were synthesized by a variant of PCR[24] involving multiple partially overlapping primers and no template DNA.[14,25] ELP$_1$ stands for the monomer of each elastin-like polypeptide, NAV stands for non-avidin biotin-binding motifs and CTRL-ELP stands for control elastin-like polypeptide that does not contain NAVs. *Deep Vent* DNA polymerase (New England Niolabs) was used in the reaction, as well as the oligonucleotide primers presented in Table S1 (Supporting Information). The detailed composition of the PCR mixture and conditions are presented in Tables S2 and S3, respectively. Four PCR reactions for either NAV-ELP$_1$ or CTRL-ELP$_1$ were performed in a *Takara Dice* PCR thermal cycler. The DNA content in PCR products was checked qualitatively by electrophoresis in 1% w/v agarose gel with 1X *GelRed* stain (Biotium) in 10 mm wells. All PCR products, either NAV-ELP$_1$ or CTRL-ELP$_1$, were combined in one sample and purified using the *QIAquick* PCR purification kit (QiaGen).

2.2. ELP Gene-Construction Step 2a—ELP$_1$ Gene Cloning in the pET29c Vector. Before proceeding to the second step of ELP gene construction (concatemerization), monomer ELP genes had to be cloned in a plasmid vector (pET29c, in this case). To facilitate this,

Downloaded from pubs.acs.org/abseba/article-pdf/7/11/5064/3413050/ab1c00329.pdf by guest on 12 November 2026

https://doi.org/10.1021/acsbiomaterials.1c00329
ACS Biomater. Sci. Eng. 2021, 7, 5064−5077

the vector and insert were digested with the restriction enzymes NdeI and KpnI. Each purified PCR product (30 μL) was diluted in ddH_2O in 43 μL final volume, followed by heat shock (incubation at 70 °C for 7 min and then incubation on ice for 7 min) and spin-down. Four reactions of 20 μL of plasmid vector diluted in ddH_2O in 43 μL final volume were also performed, followed by heat shock. 1X CutSmart buffer (New England Biolabs) was then added, and after brief spin-down, 40 U of KpnI-HF (New England Biolabs) was added with gentle mixing. In the case of digestion of the plasmid vector, reaction mixtures were incubated at 37 °C for 15 min and spun-down before being electrophorized in 1% w/v agarose gel, while inserts were digested for around 3 h. KpnI-digested DNA products were purified using the *QIAquick* PCR purification kit (QiaGen) for the inserts and using the *QIAquick* Gel extraction kit (QiaGen) for the vector. The same procedure was performed for the second digestion with NdeI (New England Biolabs). It should be noted that for both restrictive digestions, the enzyme concentration should not exceed a 10% v/v threshold to avoid star activity due to the presence of glycerol in the mixture.[26] After these digestions, vector termini were dephosphorylated by adding 1X Antarctic phosphatase buffer (New England Biolabs) and 5 U of Antarctic phosphatase (New England Biolabs), followed by 1 h incubation at 37 °C and enzyme deactivation by heating up to 70 °C for 5 min. The cloning procedure was completed by ligating the ELP_1 inserts into the linearized pET29c vector. 1X T4 DNA ligase buffer and 400 cohesive units of T4 DNA ligase (New England Biolabs) were added to 7 μL of DNA insert and 1 μL of plasmid vector, into a final volume of 10 μL. The reactions were incubated at 16 °C overnight. Cloned ELP_1 genes of the desired length (633 and 600 bp for the NAV and CTRL ELP_1 genes respectively) were selected by the transformation of competent *E. coli* TOP10 bacteria with the cloned vectors, colony screening by plasmid isolation (*QIAprep* plasmid isolation kit (QiaGen)), and NdeI-KpnI digestion, followed by agarose gel electrophoresis.

2.3. ELP Gene-Construction Step 2b—Concatemerization. The insertion of extra copies of ELP_1 monomers to derive the final ELP_3 coding genes was performed using the PRe-RDL.[15] The first step of the process is plasmid DNA isolation from recombinant *E. coli* TOP10 colonies. The procedure is as follows, and the digestion protocol is similar to the one followed for KpnI/NdeI digestions: First, eight reactions were performed where recombinant plasmids (20 μL) were digested with 5 U of BglI (New England Biolabs) (adding 1X of the appropriate buffer in a 50 μL total reaction volume). The digested products were then selected by electrophoresis in 1% w/v agarose gel and purified using the *QIAquick* Gel extraction kit (QiaGen). The digested products of the first four reactions were excised from the gel and purified using one purification column, and the digested products of the other four reactions were purified using another purification column. Afterward, the purified DNA was digested either with BseRI or AcuI (same procedure, but with the addition of 40 μM S-adenosylmethionine in the AcuI reaction). After these digestions, dephosphorylation of the AcuI-digested product followed, and plasmid fragments carrying the ELP_1 gene from both reactions were selected by electrophoresis in 0.7% w/v agarose gel; DNA was purified by gel extraction. Monoclonal ends resulting from BseRI and AcuI digestions were designed to be complementary. The reconstruction of the plasmid with the duplicated ELP (ELP_2) was performed by ligation of the two fragments using a similar procedure described in the previous paragraph. The construction of the final ELP_3 was performed by another round of PRe-RDL, ligating an ELP_2 gene and an ELP_1 gene using the same procedure. Final products were inserted into competent *E. coli* BL21 (DE3) bacteria to proceed into protein overexpression and purification.

2.4. ELP Overexpression. For the production of the NAV-ELP and CTRL-ELP proteins, transformed *E. coli* BL21 (DE3) bacteria were used as a heterologous overexpression system. Bacterial growth was performed in the Luria Bertani (LB)[27] growth medium (1% w/v tryptone, 0.5% w/v yeast extract, 1% w/v NaCl, and 1 mM NaOH) in the presence of 50 μg/mL kanamycin as the selection antibiotic. To determine the optimal conditions of growth before and after ELP-overexpression induction, we performed a series of medium-scale liquid cultures. After screening multiple different conditions using sodium dodecyl sulfate−polyacrylamide gel (SDS-PAGE) and by anti-His tag antibody Western blotting, we concluded into the following cultivation protocol: In 2 L bacterial culture flasks, 500 mL of LB/kanamycin is inoculated with ELP-transformed bacterial cells grown in short-scale liquid cultures, in 2:1000 proportion, following incubation in a shaking incubator, at 37 °C and 120 rpm shaking until OD_{600} = 0.4 for the NAV-ELP and OD_{600} = 0.6 for the CTRL-ELP. At these points of growth, plasmid overexpression is induced by adding 1 mM IPTG (Apollo Scientific), and the cultures are further incubated overnight at 22 °C under 120 rpm shaking.

2.5. ELP Purification Step 1—Organic Extraction. Cells were collected after incubation by 15 min centrifugation at 4000 rpm and 4 °C, and the cell pellet was resuspended in pH 7.5 lysis buffer (∼1 g cells in 15 mL) containing 10 mM Tris, 150 mM NaCl, and 6 M urea. In the NAV-ELP cell suspension, 1% v/v β-mercaptoethanol was also added to prevent aggregation due to the presence of Cys residues in the NAV motifs. Cell lysis was performed by sonication, with 15 cycles of 10 s ultrasound pulses of 50% intensity and 20 s pause, in the cold environment.[28] Cell lysates were centrifuged for 10 min at 4000 rpm at 4 °C. Samples from both NAV-ELP and CTRL-ELP lysates were collected for SDS-PAGE analysis.[29] SDS-PAGE gels were stained using the blue−silver staining method.[30] The first step of ELP purification was organic solvent extraction,[17,31] a method to nonchromatographically purify highly hydrophobic proteins; it was found by screening experiments that the optimal extraction of the ELPs in question could be achieved using a 1:4 cell lysate to organic solvent proportion, with the optimal solvent mixtures being acetonitrile:ethanol 3:1 for the NAV-ELP and methanol:n-butanol 1:1 for the CTRL-ELP. Cell lysates were separated into ∼4 mL aliquots in 50 mL falcon tubes. The organic solvent mixture (16 mL) was added, and the samples were vortexed violently for 10 s, before centrifugation at 4000 rpm for 10 min at room temperature. Salting out of unwanted proteins was performed by adding 20 mL of 100% saturated $(NH_4)_2SO_4$ and 2.4 mL of NaCl (5 M), followed by 10 s vortexing. The organic phase on the top containing the purified ELP was pipetted out, and the samples were ready for further treatment to recover the ELPs. ELPs can be recovered from the organic phase by either removing the solvents by rotary evaporation and drying under vacuum or by back-extracting into the aqueous solution. The former case could be successfully applied to the CTRL-ELP solution, in which the organic solvents have a low boiling point and can evaporate relatively easily in 37 °C. However, n-butanol residue remains in the evaporation flask, and this needs to be manually removed with a pipette (protein is precipitated), and the sample needs to be dried out using a vacuum pump. In the case of NAV-ELP, liquid recovery was the only feasible option. In the ELP−organic solvent solution, half volume of pH 7.5 buffer containing 10 mM Tris, 150 mM NaCl, and 0.1% v/v β-mercaptoethanol was added, along with four volumes of ethyl acetate. The mixture was vortexed, the organic phase was pipetted out, and the aqueous phase was collected. Afterward, the aqueous phase containing the ELP was dialyzed against NPI-10 buffer (*Protino* Ni-NTA protein-purification kit, Macherey-Nagel) for further purification by nickel−nitrilotriacetic acid (Ni-NTA) affinity chromatography.

2.6. ELP Purification Step 2—Ni-NTA Affinity Chromatography. Further purification of both ELPs was conducted by Ni-NTA affinity chromatography utilizing the His_6-tag of the ELPs.[32−35] For this process, *Protino Ni-NTA* 50% resin (Macherey-Nagel) was used, performing the standard gravity flow purification protocol suggested by the company. The addition of a His-tag is a well-known strategy to enable the isolation of recombinant proteins by metal-affinity chromatography and increase protein purity from crude cell lysates. Because of the relatively small size of the His_6-tag compared to the entire protein, it does not significantly interfere with the function and structure of most proteins.[36,37] Usually, the removal of His tags is strongly recommended in structural studies of recombinant proteins. However, there are studies pointing out the negative influence of the His-tag on protein stability.[38] It should be noted that the initial equilibration of the Ni-NTA column was performed by adding 10

Downloaded from pubs.acs.org/abseba/article-pdf/7/11/5064/3413050/ab1c00329.pdf by guest on 12 November 2026

https://doi.org/10.1021/acsbiomaterials.1c00329
ACS Biomater. Sci. Eng. 2021, 7, 5064−5077

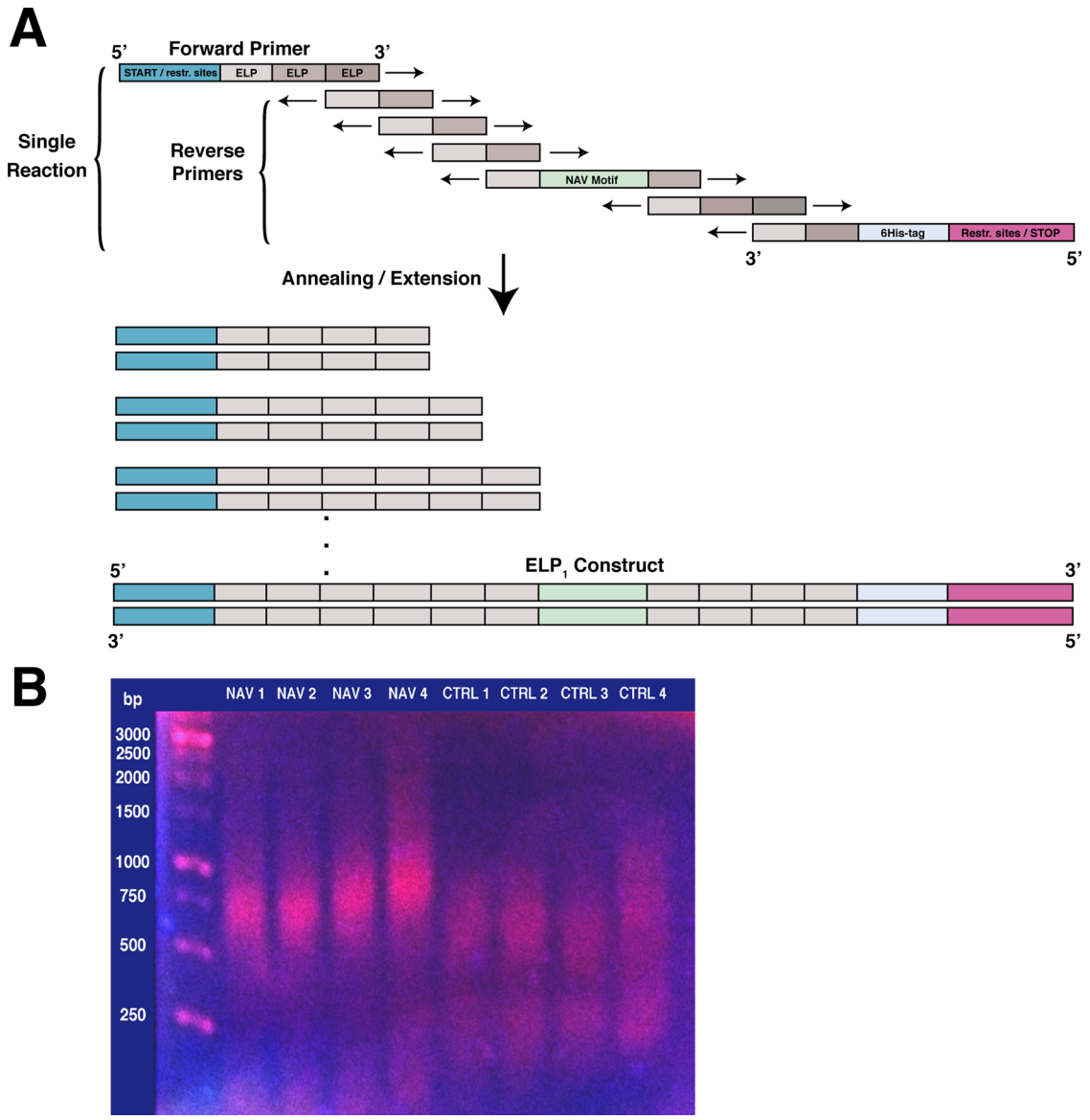


Figure 2. PCR-based gene synthesis. (A) Method principle. Partially overlapping primers (one forward primer and several reverse primers) are added in a single PCR reaction, and by adjusting the annealing temperature in each PCR cycle, specific primers gradually elongate the product. Using this method, a library of genes of various lengths is produced. (B) Electrophoresis of products from four PCR reactions for the synthesis of monomer ELP genes. Note that no distinct bands appear; this is because multiple DNA chains of different lengths are present in the final PCR product.

volumes of NPI-10 buffer containing 10 mM imidazole to the resin, followed by two steps of washing after protein binding with the NPI-20 buffer containing 20 mM imidazole, while ELPs were eluted with NPI-500 buffer containing 500 mM imidazole. Samples of all fractions were kept for SDS-PAGE analysis and Western blotting. Imidazole was removed from the purified ELP solutions by dialysis in pH 7.5 buffer containing 10 mM Tris and 150 mM NaCl (plus 0.1% v/v β-mercaptoethanol in the NAV-ELP solution). Protein band intensities in SDS-PAGE or the Western blotting membrane were estimated using the ImageJ image analysis software to calculate the purity of each ELP after organic extraction or Ni-NTA purification. Purified proteins were aliquoted and could be stored at −80 °C for up to 12 months or lyophilized for long-term storage. Lyophilization is a well-known and common process to concentrate protein samples without altering the protein properties. In addition, prior to lyophilization, the purified proteins were dialyzed extensively against deionized water to remove salts; therefore, the lyophilization process is not expected to alter the functionality of the produced protein because of the increasing concentration of charged ions during the water-removal process. The mass (in milligrams) of the lyophilized ELPs was quantified on a high-precision balance.

2.7. Preparation of ELP−Collagen Scaffolds and L929 Mouse Fibroblast Cultures on ELP−Collagen Scaffolds. Wells of a polystyrene tissue-culture (TC)-treated 96-well culture plate were coated for 2 h with 2 mg/mL type II collagen at 37 °C before being washed twice with sterile PBS 1x. Afterward, the wells were also coated with 0.5 mg of CTRL-ELP or 0.5 mg of NAV-ELP in 100 μL of sterile ddH_2O at 37 °C and incubated for 3 days, followed by washing twice with sterile PBS 1x in the final step. To evaluate the compatibility of the produced ELPs with eukaryotic cells, the L929 mouse fibroblast cell line (ECACC 85011425) was used. According to Wang, et al. (2013).[39] cytotoxicity tests often utilize the L929 cell line, which is more resistant to the toxicity of various test compounds, and therefore, we adopted the proposed protocol for the primary investigation of the toxicity. Cells (5×10^3) were inoculated onto the prepared ELP−collagen substrates in growth medium Dulbecco's modified Eagle medium (DMEM) in the presence of 10% v/v fetal bovine serum (FBS) and 2 mM glutamine. Cell growth was

Downloaded from pubs.acs.org/abseba/article-pdf/7/11/5064/3413050/ab1c00329.pdf by guest on 12 November 2026

https://doi.org/10.1021/acsbiomaterials.1c00329
ACS Biomater. Sci. Eng. 2021, 7, 5064−5077

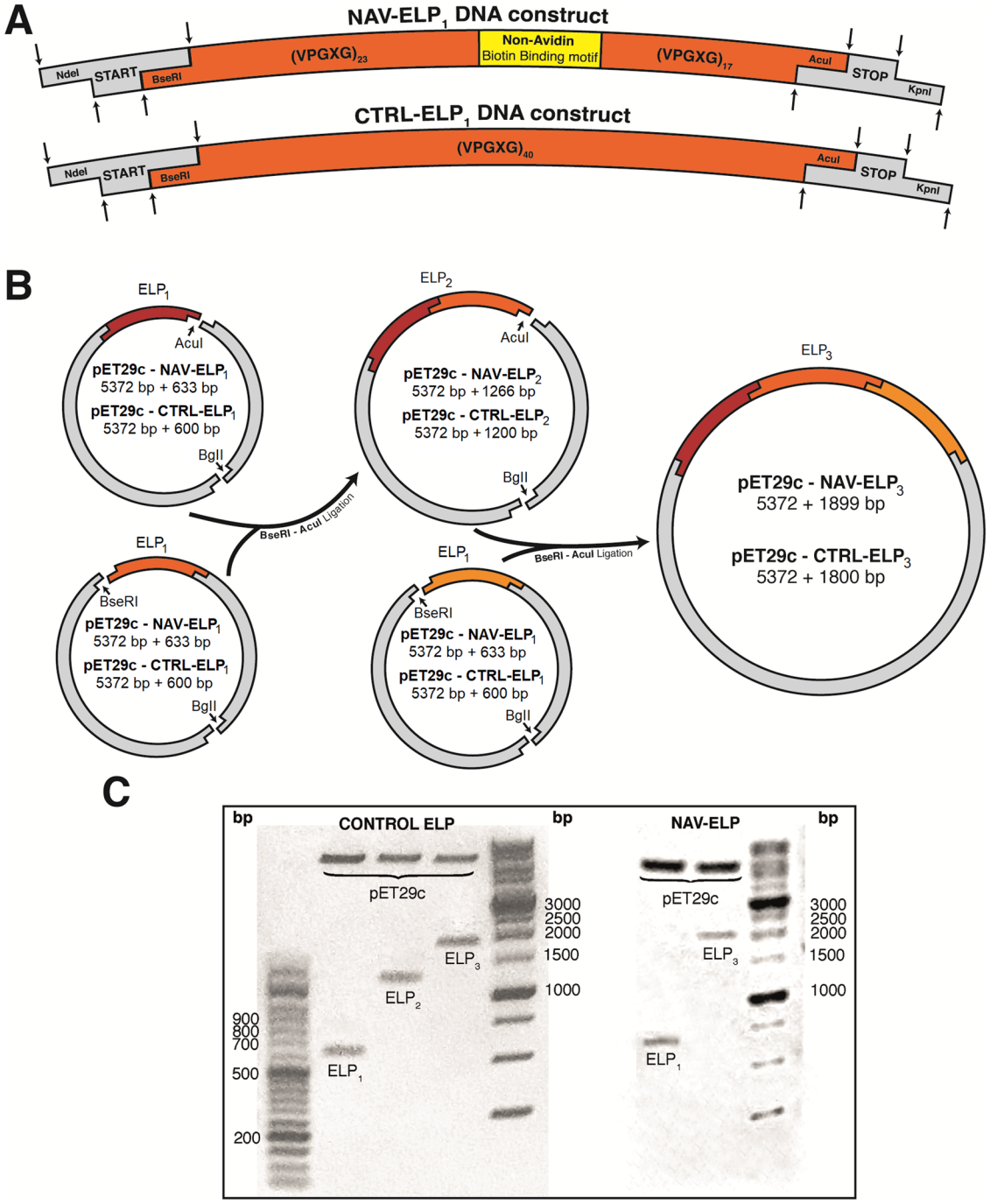


Figure 3. Recursive directional ligation by plasmid reconstruction (PRe-RDL). (A) Monomer ELP constructs to be multiplied by PRe-RDL. The constructs differ in that the NAV-ELP contains a biotin-binding motif, whereas the CTRL-ELP does not contain it. (B) Schematic procedure of Pre-RDL. With a series of restriction enzyme digestions (the exact enzymes and their cleavage sites are indicated with arrows), it is possible to introduce multiple copies of a monomer gene in a directed manner. (C) Agarose gel electrophoresis of the artificial genes during the steps of PRe-RDL. It is evident that in each cycle of PRe-RDL, an additional copy of the gene is introduced. Note that in the case of NAV-ELP, only the initial (ELP_1) and final (ELP_3) products are presented in the figure.

conducted at 37 °C under 5% v/v CO_2 in the surrounding environment.

2.8. 3-(4,5-dimethylthiazol-2-yl)-2,5-diphenyltetrazolium Assay. The 3-(4,5-dimethylthiazol-2-yl)-2,5-diphenyltetrazolium (MTT) assay is a quantitative method of measuring the metabolic activity of eukaryotic cells, hence estimating their viability.[40] The biochemical principle behind MTT is the reduction of MTT by the mitochondrial enzyme succinate dehydrogenase of metabolically active cells. The assay protocol we performed is as follows: cell suspension corresponding to 5000 cells was distributed to four 96-well plates (Corning), which were used for different incubation times. Each plate was prepared as follows: in four wells, no scaffold was added (control group), four wells were coated with 0.2 mg of type II collagen (collagen group), four wells were coated with 0.2 mg of type II collagen and 0.2 mg of purified NAV-ELP protein (NAV-ELP group), and four wells were coated with 0.2 mg of type II collagen and 0.2 mg of purified CTRL-ELP (CTRL-ELP group). Each plate was incubated for different periods (24 h, 72 h, 7 d, and 14 d). After incubation, the cell medium was discarded, and cells were rinsed gently with PBS. MTT (Sigma Aldrich) was dissolved in PBS in 5

Downloaded from pubs.acs.org/abseba/article-pdf/7/11/5064/3413050/ab1c00329.pdf by guest on 12 November 2026

https://doi.org/10.1021/acsbiomaterials.1c00329
ACS Biomater. Sci. Eng. 2021, 7, 5064−5077

Table 1. Calculated Physicochemical Parameters of the Two ELPs

polypeptide	length (residues)	M_W (kDa)	isoelectric point	hydrophobicity (aliphatic index[45])	hydrophobicity (GRAVY index[46])
NAV-ELP	658	56.05	10.88	103.9	0.92
CTRL-ELP	625	52.14	11	107.5	0.97

mg/mL concentration, and 200 μL of the solution was added in each cell well, following incubation for 3 h. The MTT solution was then discarded, and 200 μL of DMSO (100%) was added to dissolve the formazan crystals. Samples were incubated for 1 h before measuring the optical density at 570 and 630 nm in a plate spectrophotometer (Biotek). The MTT assay involves the conversion of water-soluble dye MTT to an insoluble purple formazan by the action of mitochondrial reductase of live cells. The concentration of the produced formazan is determined by measuring the optical density at 570 nm.[41] Results were recorded and statistically analyzed by calculating the mean and the standard deviation (SD).

2.9. Detection of Biotinylated GFP Bound to NAV-ELP. Wells of a polystyrene TC-treated 96-well culture plate were coated overnight with either 34 μg of GFPemerald, 100 μg of CTRL-ELP, or 100 μg of NAV-ELP in 100 μL of TBS (20 mM Tris, 150 mM NaCl, pH 7.5) at 4 °C. These wells were blocked with 5% w/v skimmed milk powder in TBS for 2 h at room temperature with gentle shaking. Wells were washed two times with TBS-T (20 mM Tris, 150 mM NaCl, 0.1% v/v Tween-20, pH 7.5). Biotinylated GFPemerald (34 μg)[22,23] in TBS was added to wells that were previously coated with CTRL-NAV or NAV-ELP, followed by an overnight incubation at 4 °C with gentle shaking. The wells were washed twice with TBS-T. Rabbit anti-GFP monoclonal antibody (Cell Signaling Technology) was added to all wells at 1:1000 dilution in TBS-T, and an overnight incubation at 4 °C with gentle shaking was followed. The wells were washed three times with TBS-T. The wells were incubated with goat anti-rabbit IgG antibody conjugated with alkaline phosphatase (Cell Signaling Technology) at 1:1000 dilution in TBS-T for 2 h at room temperature with gentle shaking. The wells were washed three times with TBS-T. Lastly, nitroblue tetrazolium (NBT) and 5-bromo-4-chloro-3-indolyl phosphate (BCIP) were added the in alkaline phosphatase buffer (100 mM Tris, 100 mM NaCl, 5 mM $MgCl_2$, pH 9.5) at a final concentration of 0.25 mg/mL for the color detection of alkaline phosphatase activity.

3. RESULTS

3.1. ELP Artificial Gene Construction. Two ELP-coding genes of ∼1800 bp were synthesized, which differ in the presence of three copies of 33 bp (11 aa) sequence coding for a NAV[18] (NAV motif: CSWRPPFRAVC), which can be potentially used as a docking site for biotinylated protein factors on the ELP peptide. The two genes and gene products will be referred as NAV-ELP and CTRL-ELP from now on, for the ELP that contains the NAV motif and the NAV-free ELP, respectively. In addition to the presence of this motif, the sequence of the two ELPs is the same, and they were designed so that they share a similar molecular weight. The final artificial genes were formed by introducing three copies of a monomer ELP gene via concatemerization. The purpose of constructing the CTRL-ELP was to use it as a negative control to test the ability of the NAV-ELP final polypeptide to bind a biotinylated protein specifically.

Monomer genes (NAV-ELP_1, CTRL-ELP_1) were synthesized using a variant of PCR in which no template DNA is required, but instead, a library of multiple partially overlapping DNA primers (one forward and multiple reverse) is used in a single reaction to progressively build up the gene in each PCR iteration.[14,25] Primer sequences are presented in Table S1 of the Supporting Information. Primers code VPGXG motifs, where X residue is either Val or Lys, with Lys residues being used to facilitate the cross-linking of the ELP peptides to form a hydrogel. Also, restriction sites are introduced in certain primers, as well as the 11aa NAV motif-coding sequence (in the NAV gene only), stop codons, and a 6His-tag. Panel A of Figure 2 illustrates the principle of the PCR-based synthesis, while the PCR products after agarose gel electrophoresis are presented in Panel B of the same figure. This technique produces a library of PCR products of various lengths; thus, no distinct bands can be seen during electrophoresis, but instead, there is a distributed smear with increased density between 500 and 1000 bp height. The selection of the monomer gene of the desired length (∼600 bp) is performed through cloning in a plasmid vector (pET29c), colony selection, and digestion via restriction enzymes.

Concatemerization of monomer ELP genes into the final ∼1800 bp genes was performed with a plasmid cloning-based technique known as PRe-RDL.[15] The technique is presented schematically in Figure 3.

Panel A of Figure 3 shows the monomer ELP constructs that were selected from the PCR-derived library, with restriction sites being indicated with arrows. Panel B shows the steps of the PRe-RDL used in this procedure. Consecutive restrictive digestions were performed on two identical pET29c vectors that carry the monomer ELP_1 genes with two pairs of restriction enzymes: AcuI-BglI and BseRI-BglI for the first and second vectors, respectively. After selecting the correct plasmid fragments from each reaction via electrophoresis, these were ligated back to reconstruct a plasmid vector carrying a duplicated ELP gene (ELP_2). This process was repeated to ligate the ELP_2 insert (1266 and 1200 bp for the NAV-ELP_2 and CTRL-ELP_2, respectively) with an ELP_1 insert so that the final ELP_3 genes are made up (1899 and 1800 bp for the NAV-ELP_2 and CTRL-ELP_2, respectively). Gene sizes refer to the actual ELP-coding sequences, without including the upstream and downstream restriction sites (BseRI and AcuI, respectively). Panel C shows the screening results of each step of PRe-RDL after KpnI-NdeI digestion and agarose gel electrophoresis. Inserts have the predicted size after each copy insertion.

3.2. Calculated Polypeptide Physicochemical Parameters. The resulting constructs from the procedures described in previous paragraphs code for two ELPs, NAV-ELP and CTRL-ELP of lengths (residues) 658 and 625, respectively. The reason for the high total amount of amino acids of the final ELPs, and therefore the high molecular mass of each ELP, is that when the molecular mass of an ELP is high, the phase-transition critical temperature is expected to be low.[42] Evidently, the number of NAV motif copies in the final NAV-ELP will be more than one because the monomer contains one copy of the NAV motif. However, the monomer gene of the NAV-ELP could have been concatenated with the monomers of CTRL-ELP, but that could be done in the future. The NAV-ELP carries three copies of 11 residue-long NAV[18] scattered in the whole length of the polypeptide sequence, while these motifs are absent from CTRL-ELP. The sequences of the two polypeptides were determined by the in silico translation of their respective DNA-coding sequences and are

Downloaded from pubs.acs.org/abseba/article-pdf/7/11/5064/3413050/ab1c00329.pdf by guest on 12 November 2026

https://doi.org/10.1021/acsbiomaterials.1c00329
ACS Biomater. Sci. Eng. 2021, 7, 5064−5077

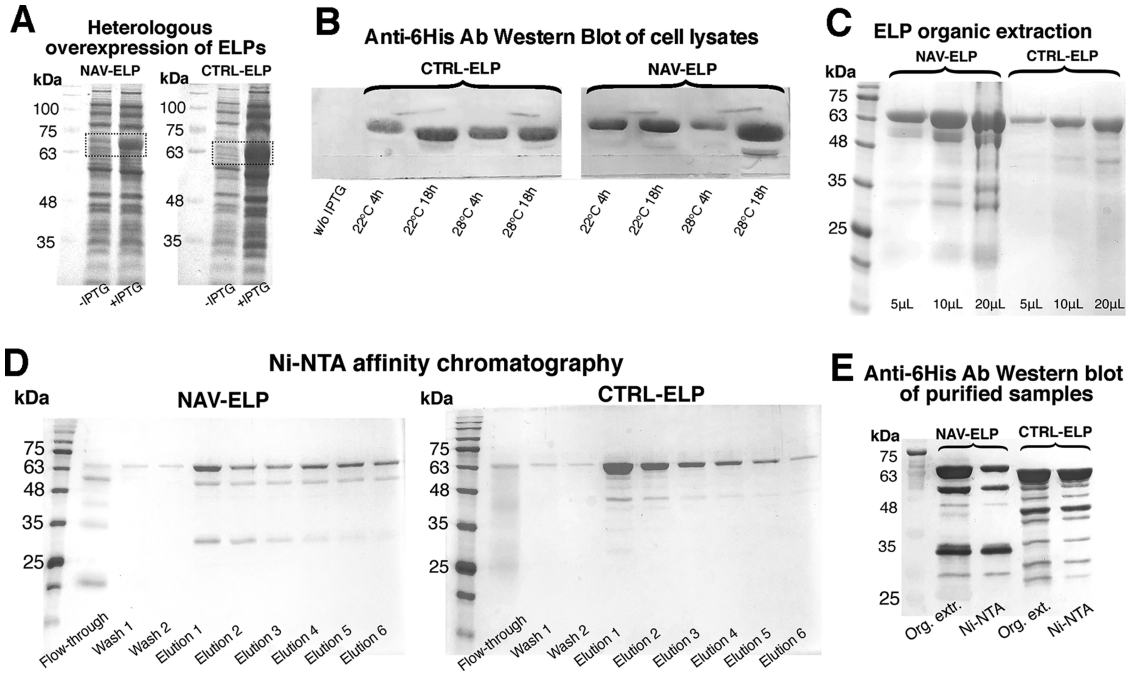


Figure 4. ELP overexpression and purification results. (A) SDS-PAGE of ELP-transformed *E.coli* BL21-DE3 cell lysates before and after overexpression induction with 1 mM IPTG. Dotted rectangles indicate the bands corresponding to the NAV-ELP and CTRL-ELP that appear after induction. (B) Anti-His_6 antibody Western blot of ELP culture cell lysates to determine optimal cultivation conditions. Dark-colored bands correspond to the His_6-tagged ELPs with the band intensity being proportional to the overexpression yield. (C) SDS-PAGE of the two ELPs in aqueous buffer, after organic extraction (first purification step). Different sample quantities were electrophorized (5, 10, and 20 μL) to assess the contaminants that remained after purification. (D) SDS-PAGE of the two ELPs after Ni-NTA affinity chromatography (second purification step). Fractions of the procedure are labeled accordingly. For each fraction of the eluted ELPs, 15 μL of 400 μL elution volume has been loaded for SDS electrophoresis. Loading an equal volume instead of an equal amount was preferred in order to follow ELP qualitative elution. It is evident that all remaining contaminants from the first purification step are cleared out in the flow-through fraction. E: Anti-His_6 antibody Western blot of the purified ELPs after organic extraction and Ni-NTA purification. Multiple bands suggest the presence of C-terminal ELP fragments, resulting from partial proteolysis during overexpression. Note that bands are much crisper in the second purification step, and with a pattern consistent with the one observed in the SDS-PAGE results of Ni-NTA chromatography (elution fractions), proving that all proteins present in the final product are ELPs without contaminants.

presented in the FASTA format, as shown in Table S4 of the Supporting Information, with certain residues and subsequences (i.e., VPGXG motifs, Lys residues, and NAV motifs) being color-coded for better visualization. Physicochemical parameters for the two polypeptides were also computed using the raw protein sequences as input to the ProtParam[43] tool of the ExPASy[43,44] platform. These are presented in Table 1. High aliphatic[45] and GRAVY[46] indices suggest that both polypeptides are highly hydrophobic, as expected in all ELPs. High hydrophobicity favors reversible self-assembly into insoluble aggregates, a definitive characteristic of ELPs, and also allows solubility in organic solvents that can be used in ELP purification. Moreover, solubility in solvents of neutral pH is possible because of the high isoelectric point (~11) of both ELPs.

3.3. Peptide Overexpression—Purification. Heterologous overexpression of the two ELPs was performed in liquid cultures of the BL21-DE3 *E. coli* strain, which was transformed by inserting the ELP recombinant pET29c plasmid vectors. Panel A of Figure 4 shows PAGE electrophoresis results of cell lysates before and after induction with 1 mM isopropyl ß-D-1-thiogalactopyranoside (IPTG). It is evident that distinctive bands appear at ~68 and ~63 kDa heights[47] for the NAV-ELP and CTRL-ELP cultures, respectively, which correspond to the overproduced ELPs. Optimization of the process to achieve maximum yield was performed through trials of different cultivation parameters (temperature after induction, IPTG induction point, time of incubation). Screening of each parameter was performed through Western blotting using anti-His_6 mouse antibody that identifies the ELPs by recognizing the C-terminal His_6-tag. Some representative results of culture condition screening (temperature and incubation time after induction) are presented in Panel B of Figure 4. The intensity of Western blot bands reflects the protein-production yield, and it was found that for both ELPs, the ideal conditions are 18 h of cultivation after IPTG induction at 22 °C. The lysis of the cells was performed by sonication under denaturing conditions (6 M urea).

An effort was made to purify the ELPs by inverse transition cycling (ITC) by the addition of a salting-out agent, as previously reported,[48] but in our case, it was not feasible by fractional precipitation and addition of a salting-out agent such as ammonium sulfate. First, both ELPs were precipitated in more than one fraction; second, the ELPs were precipitated even by the addition of a small amount of the salting-out agent; and third, many other proteins of *E. coli* were also precipitated by the addition of a small amount of the salting-out agent (data not shown). The finding that both ELPs were precipitated even by the addition of a small amount of a salting-out agent seems reasonable because both contain many hydrophobic residues on their surface (~37% of amino acids in both ELPs are hydrophobic, see also Table S4, with amino-acid sequences

Downloaded from pubs.acs.org/abseba/article-pdf/7/11/5064/3413050/ab1c00329.pdf by guest on 12 November 2026

https://doi.org/10.1021/acsbiomaterials.1c00329
ACS Biomater. Sci. Eng. 2021, 7, 5064−5077

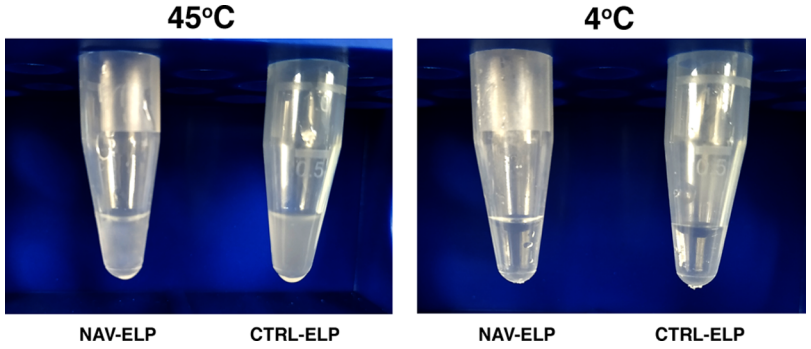


Figure 5. Temperature-dependent phase transition of the two produced ELPs. The concentration of both ELPs was 1 mg/mL. In aqueous buffer without the presence of reducing agents, ELPs can undergo reversible-phase-transition forming insoluble aggregates when samples are heated up to 45 °C, with the solutions appearing turbid (left panel). Solubility is recovered when temperature drops, with the solutions becoming transparent again (right panel).

shown in the Supporting Information). Therefore, we had to seek a nonchromatographic method, other than ITC, for the rapid purification of both ELPs. Organic solvent extraction has been utilized to purify highly hydrophobic proteins, such as intrinsically hydrophobic ELPs.[17] The purification of the ELPs was carried on in two steps to achieve the maximum possible purity while maintaining sufficient yield: organic extraction[17,31] and affinity chromatography. Organic extraction is a promising and fast technique for highly hydrophobic proteins such as ELPs that are soluble in certain organic solvents, while less-hydrophobic proteins are rendered insoluble and precipitate, making their separation easy with simple centrifugation. A series of organic solvents and their mixtures were screened for their effectiveness in extracting the ELPs with sufficient yield and purity percentage. It was found that acetonitrile:ethanol 3:1 and methanol:n-butanol 1:1 performed best in extracting the NAV-ELP and CTRL-ELP, respectively. Panel C of Figure 4 shows electrophoresis results after transferring the dissolved ELPs in the aqueous buffer (see organic solvent extraction process in the Methods section). The calculated molecular mass for NAV-ELP and CTRL-ELP is around 56 and 52 kDa, respectively (Table 1). However, the main bands are observed at around 63 kDa in SDS-PAGE (Figure 4A,C,D). It should be noted that fibrous proteins such as ELPs exhibit anomalous electrophoretic mobility in SDS-PAGE relative to protein markers.[48] Therefore, SDS-PAGE should not be relied upon to estimate the molecular mass of an ELP. Nevertheless, mass spectrometry could be performed in the future to precisely determine the molecular mass of each protein band. Using SDS-PAGE, it was observed that approximately 40 and 75% purity for the NAV-ELP and CTRL-ELP, respectively, were achieved using the organic extraction step. The appearance of the proteolysis products that decrease the percentage of purity is probably attributed to the instability of the inserted NAV motif that possesses the sequence CSWRPPFRAVC that has been computed with bioinformatics tools to be 61.62. This classifies the protein as unstable. It should be noted that high-density bands in addition to the main 68 and 63 kDa ones (NAV-ELP and CTRL-ELP, respectively) most probably correspond to C-terminal proteolysis fragments, and these byproducts are not included in the purity percentages. The inclusion of these fragments in the calculations would yield a seemingly higher percentage, but we feel that purity should only refer to the main ELP products and not include byproducts like fragments. Especially for the CTRL-ELP, the purity achieved by organic extraction could be considered sufficient; however, an extra chromatographic step would yield better results. The results of Ni-NTA affinity chromatography are presented in Panel D of Figure 4. It is evident that this extra step of purification is successful in removing the remaining contaminants from the organic extraction step, as seen from the crisp bands in the elution fractions. Moreover, minimum loss of the ELP product is observed during the washing steps, while all contaminants recede in the flow-through fraction. Finally, to cross-validate that all bands seen after purification correspond to ELPs, even if these are products of partial proteolysis, we performed Western blot of the purified ELP samples using anti-6His mouse antibody. Before performing Western blot, all elution samples of either NAV-ELP or CTRL-ELP were combined in one sample for NAV-ELP and one sample for CTRL-ELP. As seen in Panel E of Figure 4, there is a pattern of bands which is consistent with the bands seen in the Ni-NTA purification results, confirming that proteolysis occurs in the ELPs. However, these products of proteolysis should not be regarded as contaminants, as ELPs are formed of tandem repeats of a linear motif, and the presence of shorter chains would not cause unwanted functions which could be caused by the aggregation of the ELPs together with other proteins of the overexpression system *E. coli*. Indeed, downstream testing of these ELPs in the presence of live cells indicated that both ELPs exhibit biocompatibility, as seen in the MTT assay results presented later. Furthermore, the detection of protein bands by the anti-6His antibody confirms the expression of the target ELPs and their proteolysis products. It would be interesting to characterize the primary sequence of these fragments by both gas-phase sequencing and mass spectrometry. The bands from the gel will be transferred onto immobilon membranes for Edman sequencing. Regarding mass spectrometry, the low molecular-weight bands will be subjected to Arg-C proteolysis (taking into account the inserted NAV peptide that contains two arginines), and the sequence will be identified accordingly.

3.4. Produced ELPs Can Undergo Temperature-Dependent Phase Transition. A structural characteristic, definitive for ELPs, is temperature-dependent phase transition from a linear disordered state to forming partially ordered β-spiral structures that can self-assemble into rigid, insoluble aggregates. This transition of ELPs happens after surpassing critical temperature T_t, which depends on the ELP length, chemical composition, (hydrophobic group content and the kind of residues present in the guest position X of the VPGXG tandem repeat motif), solution salinity, and presence of

Downloaded from pubs.acs.org/abseba/article-pdf/7/11/5064/3413050/ab1c00329.pdf by guest on 12 November 2026

https://doi.org/10.1021/acsbiomaterials.1c00329
ACS Biomater. Sci. Eng. 2021, 7, 5064−5077

denaturing factors. This structural transition is fully reversible to the soluble state when the temperature drops below T_t, making it a useful property for the development of temperature-responsive biomaterials and in the ELP purification procedure. However, we found that organic extraction performs better for these specific ELPs designed and produced during this work. During the production and purification of the two ELP molecules, phase transition was assessed after every step of the procedure to determine whether this endogenous property is retained during the various physical−chemical treatment stages. The process was fairly simple and straightforward, including heating of 100 μL of aqueous (10 mM Tris, 150 mM NaCl, pH 7.5) ELP samples of concentration 1 mg/mL up to 45 °C, a high enough temperature to surpass T_t. Phase transition was easily confirmed by an optical observation of the change in the turbidity of the sample, with turbidity significantly increasing when ELPs self-assemble into insoluble aggregates in high temperature and decreasing when temperature drops below T_t. The phenomenon is presented in Figure 5. Nevertheless, another technique that could verify the change in the turbidity could be the measurement of the optical density at 320 nm at several temperatures. Interestingly enough, the addition of 1% v/v β-mercaptoethanol in the samples prevented aggregation, and ELPs maintained their solubility even at very high temperatures. This observation agrees with a previous report[48] that in order to visualize undenatured ELPs, buffers without β-mercaptoethanol should be used.

3.5. ELP Compatibility with Mammalian Cells. After the second purification step of the two ELP molecules using the Ni-NTA column, we performed a test of the polypeptides to assess their compatibility with eukaryotic cells. Because the future purpose of these ELPs is to function as components of tissue-engineering scaffolds, cell viability in the ELP environment is a crucial factor to be checked. The MTT cell viability test was performed in L929 mouse fibroblast cells, cultivated on four different substrates:

i. No substrate [Cells (Control)]
ii. Type II collagen substrate (Collagen)
iii. Type II collagen substrate + NAV-ELP (Col + NAV-ELP)
iv. Type II collagen substrate + CTRL-ELP (Col + CTRL-ELP)

Samples were incubated for 24 h, 72 h, 7 d, and 14 d and tested with the MTT assay after incubation. Figure 6 shows the results of cell viability expressed as the optical density at 570 nm. The profound observation is that all three substrates do not impede proliferation, although the growth of control cells is observed to be slightly higher at 24 h and 72 h time points compared to the cells grown on the three polymer substrates. On the 7th day, however, significant recovery was observed in the polymer-grown cells, which surpassed the growth of control cells. Out of these observations, it should be safe to infer that the two ELPs produced using the protocol presented in this work are not cytotoxic, and they even seem to favor cell growth when used as a substrate combined with type II collagen. Previous studies also propose that the combination of collagen with ELPs provide conditions required for superior cell proliferation.[49−51] It was aforementioned that apart from the main protein, other low-molecular-weight fragments were also observed. The phase-transition critical temperature, T_t, of an ELP depends on its molecular weight as well as the net

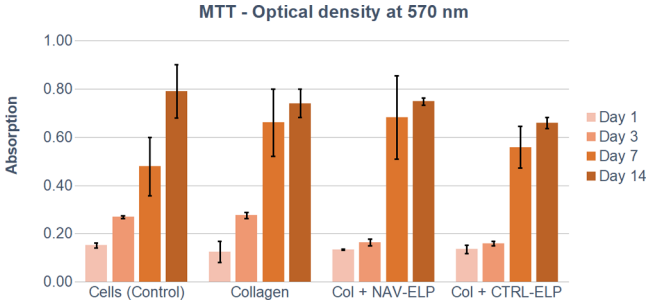


Figure 6. Results from the MTT cell viability assay in cells from the L929 mouse fibroblast cell line, cultivated in different substrates applied on the bottom of the culture wells (no substrate—control cells, type II collagen substrate, type II collagen + NAV-ELP substrate, and type II collagen + CTRL-ELP substrate). MTT assay was performed in four time points indicated by different color shades in the columns. MTT optical density was measured at 570 nm.

charge.[42] Thus, the low-molecular-weight fragments are expected to transition at a higher temperature compared to the entire ELPs. Therefore, it should be noted that in a cell culture at 37 °C, there is a possibility that only a fraction of the total ELPs may have transitioned to the aggregated state. In our experiments, the low-molecular-weight ELP aggregates have been removed by PBS washing after platting the ELPs on the collagen II matrix. Nevertheless, further studies should be conducted to strongly validate that the produced ELPs could be good candidates for cell scaffold components. As a future work, cross-linking between the side chain ε-NH_2 of the lysines introduced into the ELPs and their fragments is expected to neutralize the positive charge of the lysines at physiological pH, and therefore, an insoluble fibrous scaffold can be formed that can be then tested with various cell lines. However, this study is focused on presenting an integrated protocol for designing and producing ELP-carrying motifs for biofunctionalization, as well as a first step to test its biocompatibility and its capability to bind a biotinylated protein specifically, with characterization and downstream processes of ELP being out of its scope.

3.6. Binding of GFP to NAV-ELP. The NAV-ELP polymer was tested for its capability to bind a biotinylated protein to its biotin-binding motifs. For this purpose, biotinylated GFPemerald was utilized. In order to check if binding of a biotinylated GFP is specific, wells of a 96-well plate were coated with either GFP, CTRL-ELP, or NAV-ELP and tested for the presence of GFP using a specific antibody against GFP. To be more specific, different wells of the plate were initially treated with (1) TBS only, as the negative control, (2) GFP only, as the positive control, (3) CTRL-ELP only, as the negative control, (4) NAV-ELP, followed by the addition of biotinylated GFP, and (5) CTRL-ELP, followed by the addition of biotinylated GFP. By the color detection of alkaline phosphatase activity, as described in the Methods section, color was observed only in wells that were initially coated with either GFP or the NAV-ELP polymer (Figure 7). First, GFP would be detected by the anti-GFP antibody only when GFP was adsorbed to the surface of the well or tethered to NAV-ELP. Second, as expected, the color would be observed only when the anti-IgG secondary antibody conjugated with alkaline phosphatase would bind to the primary antibody, which, in our case, is the anti-GFP antibody. In addition, no color was observed in the wells that were coated with CTRL-ELP. As expected, in Figure 7E, the fact

Downloaded from pubs.acs.org/abseba/article-pdf/7/11/5064/3413050/ab1c00329.pdf by guest on 12 November 2026

https://doi.org/10.1021/acsbiomaterials.1c00329
ACS Biomater. Sci. Eng. 2021, 7, 5064−5077

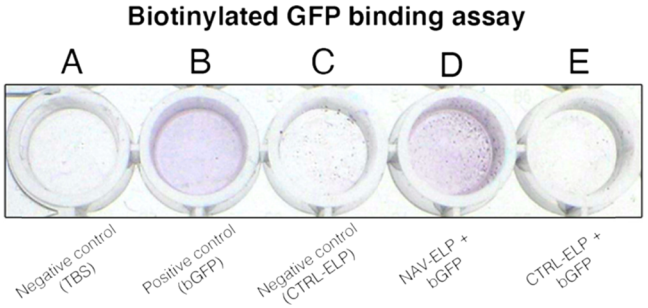


Figure 7. Binding of biotinylated GFP to biotin-binding motifs of NAV-ELP. (A) TBS only (negative control), (B) GFP only (positive control), (C) CTRL-ELP only (negative control), (D) NAV-ELP, followed by the addition of biotinylated GFP, (E) CTRL-ELP, followed by the addition of biotinylated GFP.

that no color was observed possibly indicates that GFP was washed out, and thus, it could not be detected by the anti-GFP antibody. These observations suggest that biotinylated GFP molecules were specifically bound to the biotin-binding motifs of NAV-ELP. The result described above was obtained using a qualitative method described in Methods Section 2.9. An alternative quantitative method that could be followed in the future would be the usage of a suitable substrate of alkaline phosphatase, such as *p*-nitrophenyl phosphate, and the measurement of the optical density at 405 nm.[18]

4. DISCUSSION

In this applied overview study, we design and develop a pipeline for the production of ELPs for use in regenerative medicine and drug-delivery applications. Two ELP polymers of molecular mass ∼ 60 kDa were designed, genetically synthesized, produced, purified, and partially characterized. Both peptides consist of 120 tandem repeats of the hydrophobic domain of tropoelastin VPGXG[52] and differ in the presence of three copies of a NAV motif[18] dispersed in the whole length of the ELP sequence. The ELP molecule containing these motifs is referred to as NAV-ELP, while the control ELP molecule without the motifs is referred to as CTRL-ELP. The purpose of this work is to build a reference protocol for the whole procedure of synthesizing customizable ELPs (via NAV motifs), while testing, assessing, and validating sophisticated experimental methods published in the scientific literature.

In particular, we successfully test a novel, two-step ELP gene synthesis protocol, which involves a PCR-based technique for building short-length ELP genes, without the need of template DNA, and the PRe-RDL[15] method to precisely multiply these genes by introducing the desired number of copies in a controlled manner. This combination of techniques constitutes a precise and cost-effective way to de novo-build ELP genes using minimal equipment and a set of inexpensive and easily obtainable DNA primers as raw materials. In the first gene-synthesis step, monomer ELP genes coding 36 VPGVG and 4 VPGKG copies were created. Lys-containing motifs are introduced to facilitate ELP chain cross-linking in a down-stream-processing step to build hydrogel structures. In the case of NAV-ELP, the NAV motif was inserted after the 23rd VPGXG motif. In the multiplication stage via PRe-RDL, three monomer ELP copies were concatenated to result in the final products (108 VPGVG and 12 VPGKG copies). Reviewing this combined method of gene synthesis, we deduce that it is very efficient and easily implementable for building genes consisting of tandem repeats of a motif. The PCR-based technique allows the construction of sophisticated DNA sequences, provided that the library of partially overlapping primers is designed carefully. For instance, with this PCR variant, it is possible to insert subsequences like restriction sites, purification tags, and special sequences such as the NAV motif-coding sequence.

For the efficient heterologous overexpression of the two ELP molecules, we performed a series of screening experiments to determine the optimal bacterial growth conditions and achieve maximum possible protein-production yield, while minimizing proteolysis. Cultures in the finally selected conditions were able to produce both ELPs in adequate quantity, which is evident in both cases, that is, CTRL-ELP, for which a yield was estimated ∼400 mg per 1 L of bacterial culture was achieved, while the yield of NAV-ELP was estimated ∼200 mg per 1 L of bacterial culture, after the first purification step (organic extraction). It should be noted that both yields refer to the total ELP protein. With regard to the NAV-ELP protein, overexpression levels were lower, most probably due to the presence of the NAV motifs. An observation supporting this hypothesis is the presence of two fragments of proteolysis of ∼28 and ∼50 kDa, which are also observable after the second purification step (Ni-NTA affinity chromatography). Different purity between NAV-ELP and CTRL-ELP was observed, which could be attributed to the different extents to which the proteolysis occurred between the two ELPs. Concerning NAV-ELP, we speculate that proteolysis occurs on the NAV motifs, and this might be the cause of a persistent proteolysis pattern. Proteolysis could occur at random target sequences, but the reason we speculate this in the case of NAV-ELP, where proteolysis mainly occurred on the NAV motifs, is that the two distinctive bands of ∼28 and ∼50 kDa could be attributed to the fragment until the first NAV motif and the fragment until the second NAV motif, starting from the C-terminus, whose molecular mass is calculated to be 27 and 45 kDa, respectively. In addition, the inserted NAV motif has an instability index of 61.62, as computed with bioinformatics tools, and it is classified as an unstable protein. A systematic proteolysis pattern is also seen in CTRL-ELP, in which multiple fragments are present, with a ∼45 kDa fragment being the dominant one. Currently, we cannot infer the cause of the observed proteolysis as well as the exact target sequences on which it occurs. It is known that bacteria use energy-dependent proteases to power the degradation of misfolded proteins.[53] Previous studies exhibited the presence of rescue mechanisms, such as the transfer-messenger RNA (tmRNA) system which directs nascent polypeptide chains to endogenous proteases for rapid degradation in *E. coli*.[54] In our case, the overexpression time of both ELPs could be shortened in an attempt to reduce the extent of proteolysis, but a better expression of the entire ELPs was observed after 18 h of overexpression (Figure 4B). Further investigation is mandatory to clarify the exact causes of the observed proteolysis and the target sequences on which it occurs, through peptide-sequencing experiments, mass spectrometry, and possibly as a first step, cloning of an antisense tmRNA to restrict the endogenous action of tmRNA in bacteria.

With respect to the purification procedure of the two ELPs, organic extraction has been proven very efficient for the CTRL-ELP peptide, which was purified in >70%, as observed by Western blotting. Direct recovery of the protein in the dry

Downloaded from pubs.acs.org/abseba/article-pdf/7/11/5064/3413050/ab1c00329.pdf by guest on 12 November 2026

https://doi.org/10.1021/acsbiomaterials.1c00329
ACS Biomater. Sci. Eng. 2021, 7, 5064−5077

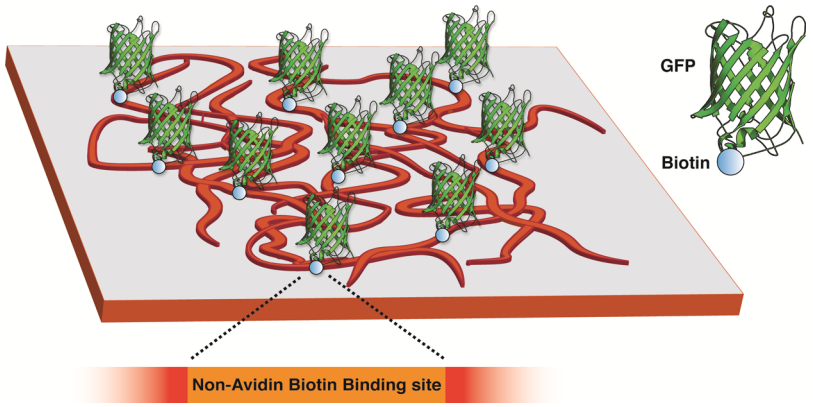


Figure 8. Schematic representation of the biofunctionalized ELP scaffold concept. ELPs carrying the NAV motif can then be biofunctionalized in a downstream process, by adding a biotinylated protein factor (GFP, in this example).

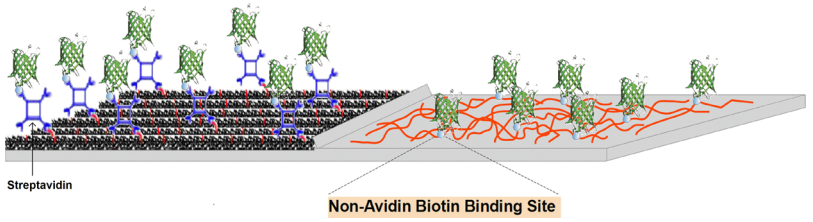


Figure 9. Comparison between biotinylated GFP bound to streptavidin and biotinylated GFP bound to a non-avidin biotin-binding motif of NAV-ELP. (Left) Initially, streptavidin is bound to a substrate comprising biotinylated polymers, and then, biotinylated GFP is bound to streptavidin via a noncovalent bond between biotin and streptavidin. (Right) Biotinylated GFP is bound to a non-avidin biotin-binding motif that is introduced genetically to the ELP scaffold without the need of streptavidin.

powder form was also possible after organic extraction (instead of back-extracting the ELP from the organic phase in aqueous buffer[17]) by rotary evaporation and vacuum drying, something that was not possible in the case of NAV-ELP because of the high boiling point of the organic solvents used. NAV-ELP could only be extracted directly to its aqueous buffer in ~35% purity. Further purity of the two peptides was achieved via Ni-NTA affinity chromatography, which was successful and resulted in significant improvement of purity. From SDS-PAGE and Western blotting results (Figure 4), it is shown that additional byproducts in the final protein solution are fragmentated ELPs due to proteolysis. The fragments can be removed, if necessary, with size exclusion chromatography.

During this work, a first step was made to characterize the NAV-ELP that was produced, in terms of its biochemical properties. Specifically, the NAV-ELP polymer was tested for its capability to bind biotinylated protein molecules to the biotin-binding motifs introduced into its amino-acid sequence. Indeed, our result indicates that NAV-ELP was able to bind biotinylated GFP specifically (Figure 7). This finding is in agreement with a previous report that explains that peptides which bear no resemblance to avidin or streptavidin can bind biotinylated proteins.[18] For future verification, the designed NAV-ELP needs to be further characterized with respect to its affinity for biotin by the measurement of binding kinetic parameters (k_{on}, k_{off}, and K_d), following a quantitative method such as enzyme-linked immunosorbent assay (ELISA). A concept of a biofunctionalized scaffold comprising the ELP polymers produced in this work is presented schematically in Figure 8.

In conclusion, in the presented work, we described in detail a cost-effective protocol for ELP synthesis and purification using known DNA-concatemerization techniques, such as PCR-based ligation[14] and Pre-RDL,[15] as well as a non-chromatographic method for the rapid purification of ELPs by organic solvent extraction.[17] Our experiments, described within this article, were focused on ELP biocompatibility as well as on their acquired properties—after the genetic insertion of the specific sequence CSWRPPFRAVC (NAV sequence)—to "allow" the interaction of biotinylated proteins or peptides without the creation of a "binding sandwich" (biotin–streptavidin–biotin). Thus, the use of tetrameric protein streptavidin that, under some conditions, would be unstable and subsequently not functional is avoided, and the desired immobilization depends only on the inserted specific sequence, as presented in Figure 9. Taking this a step further, those biotin-binding motifs could be tested as binding sites for a biotinylated factor that promotes cell differentiation and proliferation, such as the growth factors of the transforming growth factor-β (TGF-β) family, which are responsible for differentiating progenitor cells to cartilagenous tissues.[55,56] In our experiments, GFP was used as a "model" protein to study the immobilization process using the biotin-binding motifs (Figure 9). GFP is a high-molecular-weight protein (26.9), and its function is quite easy to be followed. Namely, its intrinsic fluorescence is directly proportional to a functional folding. In addition, the used GFP is endowed genetically with biotin, which recognizes a sequence avidin/streptavidin analog. In particular, we tested both the functionality of the protein as well as its ability to recognize the inserted sequence; therefore, we believe that any other protein-possessing biotin is also expected to behave similarly.

Regarding the toxicity of the NAV sequence it is clearly shown from the cytotoxicity MTT experiments that the NAV sequence is not cell lethal or cell growth inhibitor. In particular, the cytotoxicity results are very encouraging, as both ELPs

Downloaded from pubs.acs.org/abseba/article-pdf/7/11/5064/3413050/ab1c00329.pdf by guest on 12 November 2026

https://doi.org/10.1021/acsbiomaterials.1c00329
ACS Biomater. Sci. Eng. 2021, 7, 5064–5077

exhibited excellent compatibility with L929 fibroblasts in vitro, when cells were grown in rudimentary scaffolds containing type II collagen and the NAV-ELP or CTRL-ELP protein (Figure 6). In all cases, the fibroblast population was increasing over time, indicating that both NAV-ELP and CTRL-ELP are not cytotoxic. It is remarkable that when cells were grown onto plates coated with collagen only, as well as collagen and either NAV-ELP or CTRL-ELP, their population on the 7th day increased faster as compared to control fibroblasts grown on plates without coating. This observation implies that collagen alone, or a combination of collagen with ELPs, provide a better surrounding environment for cell growth.

The primary reason to use ELPs as scaffold components is their mechanical properties, such as their high elastic modulus and durability, making such scaffold-containing ELPs very suitable for developing tensile tissues like cartilages, tendons, and skin. Other studies also suggest that composites of collagen with ELP can form good-quality scaffolds with reinforced mechanical properties (tensile strength and toughness) required for tissue-engineering applications.[49−51] In addition, the genetically produced NAV-ELPs would be of great importance for creating diagnostic kits that recommend the functional immobilization of biotinylated enzymes to investigate inhibitory or enhancement properties of several compounds.

■ ASSOCIATED CONTENT

Supporting Information

The Supporting Information is available free of charge at https://pubs.acs.org/doi/10.1021/acsbiomaterials.1c00329.

Oligonucleotide sequences used for artificial gene synthesis; reaction components and conditions utilized for gene synthesis; and amino-acid sequences of the final ELP concatemers (PDF).

■ AUTHOR INFORMATION

Corresponding Author

Theodora Choli-Papadopoulou − *Laboratory of Biochemistry, School of Chemistry, Aristotle University of Thessaloniki, Thessaloniki 54124, Greece;* orcid.org/0000-0002-7459-5807; Email: tcholi@chem.auth.gr

Authors

Ioannis G. Riziotis − *Laboratory of Biochemistry, School of Chemistry, Aristotle University of Thessaloniki, Thessaloniki 54124, Greece*

Paraskevas Lamprou − *Laboratory of Biochemistry, School of Chemistry, Aristotle University of Thessaloniki, Thessaloniki 54124, Greece*

Eleni Papachristou − *Laboratory of Biochemistry, School of Chemistry, Aristotle University of Thessaloniki, Thessaloniki 54124, Greece*

Aglaia Mantsou − *Laboratory of Biochemistry, School of Chemistry, Aristotle University of Thessaloniki, Thessaloniki 54124, Greece*

Georgios Karolidis − *Laboratory of Biochemistry, School of Chemistry, Aristotle University of Thessaloniki, Thessaloniki 54124, Greece*

Rigini Papi − *Laboratory of Biochemistry, School of Chemistry, Aristotle University of Thessaloniki, Thessaloniki 54124, Greece;* orcid.org/0000-0002-3183-4724

Complete contact information is available at: https://pubs.acs.org/10.1021/acsbiomaterials.1c00329

Author Contributions

†I.G.R. and P.L. contributed equally to this work.

Notes

The authors declare no competing financial interest.

■ ACKNOWLEDGMENTS

This research was supported by the project "Synthetic Biology: From omics technologies to genomic engineering (OMIC-ENGINE)" (MIS 5002636) that was cofinanced by Greek national funds and European Union. This research has also been cofinanced by the European Regional Development Fund of the European Union and Greek national funds through the Operational Program Competitiveness, Entrepreneurship and Innovation (NSRF 2014-2020), under the call RESEARCH−CREATE−INNOVATE (project code: T1EDK-04567).

■ REFERENCES

(1) Anwar. Elastin: A brief Review. *Biochem. Educ.* **1990**, *18*, 162−166.

(2) Hu, X.; Cebe, P.; Weiss, A. S.; Omenetto, F.; Kaplan, D. L. Protein-Based Composite Materials. *Mater. Today* **2012**, *15*, 208−215.

(3) Urry, D. W.; Parker, T. M.; Reid, M. C.; Gowda, D. C. Biocompatibility of the Bioelastic Materials, Poly(GVGVP) and Its γ-Irradiation Cross-Linked Matrix: Summary of Generic Biological Test Results. *J. Bioact. Compat. Polym.* **1991**, *6*, 263−282.

(4) Urry, D. W.; Hugel, T.; Seitz, M.; Gaub, H. E.; Sheiba, L.; Dea, J.; Xu, J.; Parker, T. Elastin: A Representative Ideal Protein Elastomer. *Philos. Trans. R. Soc. B* **2002**, *357*, 169−184.

(5) Gagner, J. E.; Kim, W.; Chaikof, E. L. Designing Protein-Based Biomaterials for Medical Applications. *Acta Biomater.* **2014**, 1542−1557.

(6) Nicol, A.; Channe Gowda, D.; Urry, D. W. Cell Adhesion and Growth on Synthetic Elastomeric Matrices Containing ARG-GLY−ASP−SER−3. *J. Biomed. Mater. Res.* **1992**, *26*, 393−413.

(7) Liu, J. C.; Heilshorn, S. C.; Tirrell, D. A. Comparative Cell Response to Artificial Extracellular Matrix Proteins Containing the RGD and CS5 Cell-Binding Domains. *Biomacromolecules* **2004**, *5*, 497−504.

(8) Ruoslahti, E. RGD and Other Recognition Sequences for Integrins. *Annu. Rev. Cell Dev. Biol.* **1996**, *12*, 697−715.

(9) Gobbi, S. J. Requirements for Selection/Development of a Biomaterial. *Biomed. J. Sci. Tech. Res.* **2019**, *14*, 10674−10679.

(10) Rodríguez-Cabello, J. C.; Prieto, S.; Arias, F. J.; Reguera, J.; Ribeiro, A. Nanobiotechnological Approach to Engineered Biomaterial Design: The Example of Elastin-like Polymers. *Nanomedicine* **2006**, *1*, 267−280.

(11) Roberts, S.; Dzuricky, M.; Chilkoti, A. Elastin-like Polypeptides as Models of Intrinsically Disordered Proteins. *FEBS Lett.* **2015**, 2477−2486.

(12) Le, D. H. T.; Sugawara-Narutaki, A. Elastin-like Polypeptides as Building Motifs toward Designing Functional Nanobiomaterials. *Mol. Syst. Des. Eng.* **2019**, *4*, 545−565.

(13) Chilkoti, A.; Christensen, T.; MacKay, J. Stimulus Responsive Elastin Biopolymers: Applications in Medicine and Biotechnology. *Curr. Opin. Chem. Biol.* **2006**, *10*, 652−657.

(14) Hemat, F.; McEntee, K. A Rapid and Efficient PCR-Based Method for Synthesizing High-Molecular-Weight Multimers of Oligonucleotides. *Biochem. Biophys. Res. Commun.* **1994**, *205*, 475−481.

(15) McDaniel, J. R.; MacKay, J. A.; Quiroz, F. G.; Chilkoti, A. Recursive Directional Ligation by Plasmid Reconstruction Allows Rapid and Seamless Cloning of Oligomeric Genes. *Biomacromolecules* **2010**, *11*, 944−952.

Downloaded from pubs.acs.org/abseba/article-pdf/7/11/5064/3413050/ab1c00329.pdf by guest on 12 November 2026

(16) Girotti, A.; Fernández-Colino, A.; López, I. M.; Rodríguez-Cabello, J. C.; Arias, F. J. Elastin-like recombinamers: Biosynthetic Strategies and Biotechnological Applications. *Biotechnol. J.* **2011**, *6*, 1174−1186.
(17) Verheul, R.; Sweet, C.; Thompson, D. H. Rapid and Simple Purification of Elastin-like Polypeptides Directly from Whole Cells and Cell Lysates by Organic Solvent Extraction. *Biomater. Sci.* **2018**, *6*, 863−876.
(18) Saggio, I.; Laufer, R. Biotin Binders Selected from a Random Peptide Library Expressed on Phage. *Biochem. J.* **1993**, *293*, 613−616.
(19) McHale, M. K.; Setton, L. A.; Chilkoti, A. Synthesis and *in Vitro* Evaluation of Enzymatically Cross-Linked Elastin-like Polypeptide Gels for Cartilaginous Tissue Repair. *Tissue Eng.* **2005**, *11*, 1768−1779.
(20) Tsiapalis, D.; De Pieri, A.; Biggs, M.; Pandit, A.; Zeugolis, D. I. Biomimetic Bioactive Biomaterials: The Next Generation of Implantable Devices. *ACS Biomater. Sci. Eng.* **2017**, 1172−1174.
(21) Herrero-Vanrell, R.; Rincón, A. C.; Alonso, M.; Reboto, V.; Molina-Martinez, I. T.; Rodríguez-Cabello, J. C. Self-Assembled Particles of an Elastin-like Polymer as Vehicles for Controlled Drug Release. *J. Controlled Release* **2005**, *102*, 113−122.
(22) Chapman-Smith; Mulhern; Whelan; Cronan, J. E., Jr.; Wallace, J. C. The C-Terminal Domain of Biotin Protein Ligase from *E. coli* Is Required for Catalytic Activity. *Protein Sci.* **2001**, *10*, 2608−2617.
(23) Logothetidis, S. *Nanomedicine and Nanobiotechnology*. Nanoscience and Technology; vol *61*; Springer, 2012, DOI: 10.1007/978-3-642-24181-9.
(24) Mullis, K.; Faloona, F.; Scharf, S.; Saiki, R.; Horn, G.; Erlich, H. Specific Enzymatic Amplification of DNA *in Vitro*: The Polymerase Chain Reaction. *Cold Spring Harbor Symp. Quant. Biol.* **1986**, *51*, 263−273.
(25) Prodromou, C.; Pearl, L. H. Recursive PCR: A Novel Technique for Total Gene Synthesis. *Protein Eng., Des. Sel.* **1992**, *5*, 827−829.
(26) Lundin, S.; Jemt, A.; Terje-Hegge, F.; Foam, N.; Pettersson, E.; Käller, M.; Wirta, V.; Lexow, P.; Lundeberg, J. Endonuclease Specificity and Sequence Dependence of Type IIS Restriction Enzymes. *PLoS One* **2015**, *10*, No. e0117059.
(27) Luria, S. E.; Burrous, J. W. Hybridization Between *Escherichia Coli* and *Shigella*. *J. Bacteriol.* **1957**, *74*, 461−476.
(28) Shehadul Islam, M.; Aryasomayajula, A.; Selvaganapathy, P. R. A Review on Macroscale and Microscale Cell Lysis Methods. *Micromachines* **2017**, *8*, 83.
(29) Bonifacino, J. S. Electrophoresis and Immunoblotting. *Curr. Protoc. Cell Biol.* 2002, *15* (1), DOI: 10.1002/0471143030.cb0600s15.
(30) Candiano, G.; Bruschi, M.; Musante, L.; Santucci, L.; Ghiggeri, G. M.; Carnemolla, B.; Orecchia, P.; Zardi, L.; Righetti, P. G. Blue Silver: A Very Sensitive Colloidal Coomassie G-250 Staining for Proteome Analysis. *Electrophoresis* **2004**, *25*, 1327−1333.
(31) Yakhnin, A. V.; Vinokurov, L. M.; Surin, A. K.; Alakhov, Y. B. Green Fluorescent Protein Purification by Organic Extraction. *Protein Expression Purif.* **1998**, *14*, 382−386.
(32) Lowe, C. R. Affinity Chromatography: Principles and Applications. In *Chromatographic and Membrane Processes in Biotechnology*. 1991, pp. 289−296. DOI: 10.1007/978-94-011-3470-5_15.
(33) Bornhorst, J. A.; Falke, J. J. Purification of Proteins Using Polyhistidine Affinity Tags. *Methods Enzymol.* **2000**, *326*, 245−254.
(34) Coelho, L. C., Santos, A. F., Napoleão, T. H., Correia, M. T., Paiva, P. M. Protein Purification by Affinity Chromatography. In *Protein Purification*. IntechOpen, 2012. DOI: 10.5772/29947.
(35) Young, C. L.; Britton, Z. T.; Robinson, A. S. Recombinant Protein Expression and Purification: A Comprehensive Review of Affinity Tags and Microbial Applications. *Biotechnol. J.* **2012**, 620−634.
(36) Structural Genomics Consortium; Architecture et Fonction des Macromolécules Biologiques; Berkeley Structural Genomics Center; China Structural Genomics Consortium; Integrated Center for Structure and Function Innovation; Israel Structural Proteomics Center; Joint Center for Structural Genomics; Midwest Center for Structural Genomics; New York Structural GenomiX Research Center for Structural Genomics; Northeast Structural Genomics Consortium; Oxford Protein Production Facility; Protein Sample Production Facility, Max Delbrück Center for Molecular Medicine; RIKEN Structural Genomics/Proteomics Initiative; SPINE2-Complexes Protein production and purification. *Nat. Methods* 2008, *5*, 135−146, DOI: 10.1038/nmeth.f.202.
(37) Uhlén, M.; Forsberg, G.; Moks, T.; Hartmanis, M.; Nilsson, B. Fusion proteins in biotechnology. *Curr. Opin. Biotechnol.* **1992**, *3*, 363−369.
(38) Booth, W. T.; Schlachter, C. R.; Pote, S.; Ussin, N.; Mank, N. J.; Klapper, V.; Offermann, L. R.; Tang, C.; Hurlburt, B. K.; Chruszcz, M. Impact of an N-terminal Polyhistidine Tag on Protein Thermal Stability. *ACS Omega* **2018**, *3*, 760−768.
(39) Wang, M. O.; Etheridge, J. M.; Thompson, J. A.; Vorwald, C. E.; Dean, D.; Fisher, J. P. Evaluation of the *in vitro* cytotoxicity of crosslinked biomaterials. *Biomacromolecules* **2013**, *14*, 1321−1329.
(40) Gerlier, D.; Thomasset, N. Use of MTT Colorimetric Assay to Measure Cell Activation. *J. Immunol. Methods* **1986**, *94*, 57−63.
(41) Morgan, D.M.L. Tetrazolium (MTT) Assay for Cellular Viability and Activity. In *Polyamine Protocols*; Morgan, D.M.L., Eds.; Methods in Molecular Biology, vol *79*; Humana Press, 1998. DOI: 10.1385/0-89603-448-8:179.
(42) Rodríguez-Cabello, J. C.; Martín, L.; Alonso, M.; Arias, F. J.; Testera, A. M. "Recombinamers" as Advanced Materials for the Post-Oil Age. *Polymer* **2009**, *50*, 5159−5169.
(43) Gasteiger, E.; Hoogland, C.; Gattiker, A.; Duvaud, S.; Wilkins, M. R.; Appel, R. D.; Bairoch, A. Protein Identification and Analysis Tools on the ExPASy Server. In *The Proteomics Protocols Handbook*; Humana Press, 2005, pp. 571−607. DOI: 10.1385/1-59259-890-0:571.
(44) Gasteiger, E.; Gattiker, A.; Hoogland, C.; Ivanyi, I.; Appel, R. D.; Bairoch, A. ExPASy: The Proteomics Server for in-Depth Protein Knowledge and Analysis. *Nucleic Acids Res.* **2003**, *31*, 3784−3788.
(45) Ikai, A. Thermostability and Aliphatic Index of Globular Proteins. *J. Biochem.* **1980**, *88*, 1895−1898.
(46) Kyte, J.; Doolittle, R. F. A Simple Method for Displaying the Hydropathic Character of a Protein. *J. Mol. Biol.* **1982**, *157*, 105−132.
(47) Shapiro, A. L.; Viñuela, E.; V. Maizel, J., Jr. Molecular Weight Estimation of Polypeptide Chains by Electrophoresis in SDS-Polyacrylamide Gels. *Biochem. Biophys. Res. Commun.* **1967**, *28*, 815−820.
(48) Hassouneh, W.; MacEwan, S. R.; Chilkoti, A. Fusions of Elastin-Like Polypeptides to Pharmaceutical Proteins. *Methods Enzymol.* **2012**, *502*, 215−237.
(49) Newman, K.; Clark, K.; Gurumurthy, B.; Pal, P.; Janorkar, A. V. Elastin-Collagen Based Hydrogels as Model Scaffolds to Induce Three-Dimensional Adipocyte Culture from Adipose Derived Stem Cells. *Bioengineering (Basel)* **2020**, *7*, 110.
(50) Gurumurthy, B.; Bierdeman, P. C.; Janorkar, A. V. Composition of Elastin Like Polypeptide−Collagen Composite Scaffold Influences *In Vitro* Osteogenic Activity of Human Adipose Derived Stem Cells. *Dent. Mater.* **2016**, *32*, 1270−1280.
(51) Gurumurthy, B.; Griggs, J. A.; Janorkar, A. V. Optimization of collagen-elastin-like polypeptide composite tissue engineering scaffolds using response surface methodology. *J. Mech. Behav. Biomed. Mater.* **2018**, *84*, 116−125.
(52) Vrhovski, B.; Weiss, A. S. Biochemistry of Tropoelastin. *Eur. J. Biochem.* **1998**, 1−18.
(53) Mahmoud, S. A.; Chien, P. Regulated Proteolysis in Bacteria. *Annu. Rev. Biochem.* **2018**, *87*, 677−696.
(54) Cameron, D. E.; Collins, J. J. Tunable Protein Degradation in Bacteria. *Nat. Biotechnol.* **2014**, *32*, 1276−1281.
(55) Betre, H.; Ong, S. R.; Guilak, F.; Chilkoti, A.; Fermor, B.; Setton, L. A. Chondrocytic Differentiation of Human Adipose-Derived Adult Stem Cells in Elastin-like Polypeptide. *Biomaterials* **2006**, *27*, 91−99.

Downloaded from pubs.acs.org/abseba/article-pdf/7/11/5064/3413050/ab1c00329.pdf by guest on 12 November 2026

(56) Deng, Z. H.; Li, Y. S.; Gao, X.; Lei, G. H.; Huard, J. Bone Morphogenetic Proteins for Articular Cartilage Regeneration. *Osteoarthr. Cartil.* **2018**, 1153−1161.

Downloaded from pubs.acs.org/abseba/article-pdf/7/11/5064/3413050/ab1c00329.pdf by guest on 12 November 2026

https://doi.org/10.1021/acsbiomaterials.1c00329
ACS Biomater. Sci. Eng. 2021, 7, 5064−5077